Effect of a Dispersion of Interfacial Electron Transfer Rates on Steady State Catalytic Electron Transport in [NiFe]-hydrogenase and Other Enzymes

Christophe Léger,[†,||] Anne K. Jones,[†] Simon P. J. Albracht,[‡] and Fraser A. Armstrong*[,†]

Inorganic Chemistry Laboratory, South Parks Road, Oxford OX1 3QR, United Kingdom, and Swammerdam Institute for Life Sciences, Biochemistry, University of Amsterdam, Plantage Muidergracht 12, NL-1018 TV Amsterdam, The Netherlands

Received: July 19, 2002; In Final Form: October 4, 2002

Redox enzymes can be adsorbed onto electrode surfaces such that there is a rapid and efficient direct electron transfer (ET) between the electrode and the enzyme's active site, along with high catalytic activity. In an idealized way, this may be analogous to protein−protein ET or, more significantly, the nonrigid interface between different domains of membrane-bound enzymes. The catalytic current that is obtained when substrate is added to the solution is directly proportional to the enzyme's turnover rate and its dependence on the electrode potential reports on the energetics and kinetics of the entire catalytic cycle. Although the current is expected to reach a limiting value as the electrode potential is varied to increase the driving force, a residual slope in voltammograms is often observed. This slope is significant, as it is unexpected from all simple considerations of electrochemical kinetics. A particularly remarkable result is obtained in experiments carried out with the [NiFe]-hydrogenase from *Allochromatium vinosum*: this enzyme displays high catalytic activity for hydrogen oxidation and is easily studied up to 60 °C, at which temperature the current−potential response becomes completely linear over a range of more than 0.5 V. The explanation for this effect is that the enzyme molecules are not adsorbed in a homogeneous manner but vary in their degree of ET coupling with the electrode, i.e., through there being many slightly different orientations. Under conditions in which interfacial ET becomes rate-limiting, i.e., when turnover number is high at elevated temperatures, the current−potential response reflects the superposition of numerous electrochemical rate constants. This is highly relevant in the interpretation of the catalytic electrochemistry of enzymes.

Introduction

In catalytic protein film voltammetry[1] (PFV), a redox enzyme is adsorbed onto an electrode, typically to submonolayer coverage. Direct, long-range electron transfer (ET) occurs between the electrode and the buried active site, usually through an intramolecular chain of redox groups, such as iron−sulfur clusters or hemes, that is naturally designed to facilitate fast and efficient intramolecular ET.[2] The driving force for the catalytic reaction is provided through the applied electrode potential and can be fine-tuned, while the catalytic activity is simultaneously and precisely measured as a steady state, faradaic current that results from the continuous regeneration of the active site by interfacial ET: importantly, the magnitude of the current is directly proportional to the turnover rate. This kind of experiment presents important opportunities to study enzyme kinetics since the resulting voltammograms reveal the exact variation in activity (current) as a function of driving force (electrode potential) and contain information about the kinetics and energetics of interconversions between catalytic intermediates.[3−5] Yet, as we now describe, the nature of the interaction between the electrode and these giant catalysts is unclear and provides a further intriguing dimension to these studies.

Hydrogenases are enzymes that catalyze the evolution and oxidation of H_2 (see refs 6−10 for recent reviews). The [NiFe]-hydrogenase from the purple sulfur bacterium *Allochromatium vinosum* contains a buried active site for H_2/H^+ interconversion (the [NiFe(CO)$(CN)_2$] center), which is redox-coupled to the protein surface by a chain of three [FeS] clusters. When adsorbed onto a pyrolytic graphite edge (PGE) electrode, the enzyme displays intense catalytic activity.[11,12] The turnover number, which exceeds 1500 s^{-1} at 30 °C (ref 11), is considerably higher than that measured using soluble redox dyes as electron acceptors, indicating that in these more conventional solution experiments, the rate is limited by the reaction with the mediator. The activity of the enzyme is so high that with optimized coverage on the electrode, the hydrogen substrate is depleted near the electrode surface and mass transport-controlled voltammetry is observed, for which the catalytic current increases with the electrode rotation rate.[11] However, an interesting situation arises if the electrode surface onto which the enzyme is adsorbed is abraded; for example, with cotton wool, this greatly lowers the coverage of enzyme, and if the pressure of H_2 is increased to one bar, mass transport control is removed.[12] The influence of temperature is now strikingly revealed, and as shown in Figure 1, the quasi-sigmoidal catalytic wave observed at low temperature converts to a response that is linear over a potential range of more than 0.5 V when the temperature is raised. The linearity is unexpected and resembles that for a device obeying Ohm's law. Similar observations, albeit in most cases less dramatic,[3−5,12−20] have been made for other

* To whom correspondence should be addressed. Tel: 44-1865-272647. Fax: 44-1865-272690. E-mail: fraser.armstrong@chem.ox.ac.uk.
[†] Inorganic Chemistry Laboratory.
[‡] University of Amsterdam.
[||] Current address: Laboratoire de Bioénergétique et Ingénierie des Protéines, CNRS, Marseille, France.

10.1021/jp0265687 CCC: $22.00
Published on Web 11/20/2002

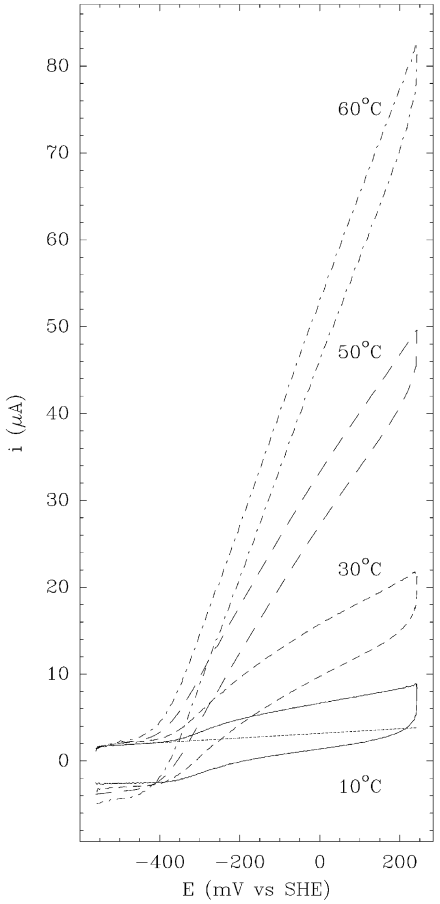

Figure 1. Catalytic hydrogen oxidation by *A. vinosum* [NiFe]-hydrogenase adsorbed at a PGE electrode at pH 7, under one bar H_2, as a function of temperature. As the enzyme activity increases, the catalytic response is transformed from a sigmoid to a line. The electrode geometric area was $A = 0.03$ cm^2, the scan rate was $\nu = 1$ V/s, and the electrode rotation rate was $\omega = 2500$ rpm. Increasing ω further produced no change in the voltammetry, showing that it is not mass transport-controlled. The dotted line shows the linear baseline that is subtracted to remove the capacitive current before fitting the data (Figure 5).

enzymes confined to an electrode surface, leading us to question its origin and mechanistic significance.

In this paper, we discuss the origin of this behavior and show that it can be explained by disorder among the adsorbed enzyme molecules, resulting in a dispersion of interfacial ET rate constants. There are interesting implications both for the interpretation of catalytic waveshapes for adsorbed enzymes and on the influence of the fidelity of intermacromolecular interactions in physiological ET reactions.

Modeling

Ideal Case. The two-electron oxidation of a substrate occurring at the redox active site of an enzyme normally involves two one-electron oxidations of the active site, followed by product formation and release and substrate binding. In classical enzyme kinetics, turnover is measured as a function of the concentrations of various reactants, whereas PFV adds the "potential dimension" to this investigation, since rates of redox processes (and therefore turnover) depend on the electrode potential. According to the Butler−Volmer model,[21,22] the rate of interfacial ET increases exponentially with the driving force (overpotential, η); consequently, the ET rate will always eventually exceed the rate of substrate conversion by the enzyme-substrate complex. According to Marcus theory,[22,23] the rate of interfacial ET starts to level off once the overpotential becomes higher than the reorganization energy of the reaction ($\eta > \lambda$). With these considerations (i.e., whatever the ET model) and assuming that the rate of substrate conversion is independent of potential, the resulting catalytic voltammogram is expected to show the current increasing with overpotential at moderate driving force and then leveling off to a limiting value (plateau).

SCHEME 1: Generic Scheme for a Two-Electron Catalytic Oxidation[a]

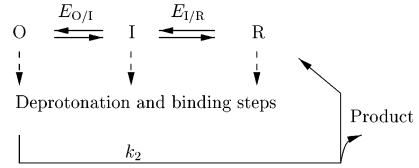

[a] The reduced form of the active site is oxidized to O (via an intermediate species I) following two one-electron transfers and coupled deprotonation steps. The oxidized, substrate-bound form of the active site makes and releases the product with a rate k_2.

In ref 5, equations were derived for the current corresponding to the steady state, catalytic, two electron oxidation of a substrate by an enzyme adsorbed on an electrode, assuming that mass transport of the substrate to the electrode is not rate-limiting. Further assumptions were that (i) the active site exists in three redox states termed O (oxidized), I (half-reduced intermediate), and R (reduced). As depicted in Scheme 1, the oxidized, deprotonated, and substrate-bound form of the active site regenerates R, while the product of the reaction is produced with a first-order rate constant k_2. (ii) (De)protonation and substrate binding steps are at equilibrium throughout. (iii) The rate of active site oxidation as a function of the electrode potential E is predicted by Butler−Volmer formalism,[21] i.e.,

$$k_{O\rightarrow I} = k_0 \exp\left[\frac{-f}{2}(E - E_{O/I})\right] = k_0 e_{O/I}^{-1/2} \qquad (1a)$$

$$k_{I\rightarrow O} = k_0 \exp\left[\frac{f}{2}(E - E_{O/I})\right] = k_0 e_{O/I}^{1/2} \qquad (1b)$$

with $e_{O/I} = \exp[f(E - E_{O/I})]$, $E_{O/I}$ is the reduction potential of the O/I couple, $f = F/RT$, and k_0 is the interfacial ET rate at zero overpotential, which is assumed to be the same for all adsorbed enzyme molecules. Analogous equations hold for the I/R transformation.

The model predicts that the current i increases from zero at low potential to a limiting value i_{lim} at high driving force according to[24]

$$\frac{i_{lim}}{i} - 1 = e_{O/I}^{-1}(1 + e_{I/R}^{-1}) + \frac{k_2}{k_0}\{e_{I/R}^{-1/2} + e_{O/I}^{-1/2}(1 + e_{I/R}^{-1})\} \qquad (2)$$

where $i_{lim} = 2FA\Gamma k_2$ (i.e., the limiting current is enzyme-controlled), A is the electrode surface area, and Γ is the electroactive coverage of enzyme. Four parameters must be adjusted to fit the data to eq 2: two reduction potentials, k_2/k_0 and i_{lim}.

Origin of Nonidealities. Because intramolecular ET along the chain of Fe−S clusters in hydrogenase is expected to be very fast,[2] we assume that the overall rate of ET depends on the distance-related electronic coupling between the electrode and the surface-exposed [4Fe−4S] cluster that provides the entry/exit point for electrons within the enzyme. The important extension of the model described above is that we now consider the effect of disorder in the orientation of enzyme molecules

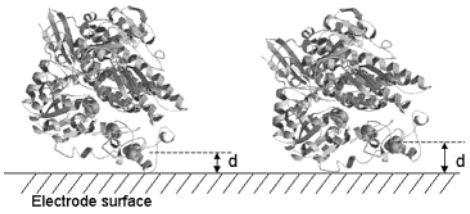

Figure 2. Cartoon illustrating the consequences of two different orientations of *A. vinosum* [NiFe]-hydrogenase on an electrode, resulting in different tunneling distances *d* for interfacial ET. In the case of *A. vinosum* [NiFe]-hydrogenase, ET occurs from the electrode surface to the enzyme active site through a "wire" of Fe−S clusters. The so-called distal [4Fe−4S] cluster is surface-exposed and is believed to be the site of interaction with a redox partner, and *d* is indicated to this center. The structure shown is that of *Desulfovibrio gigas* [NiFe]-hydrogenase.[25]

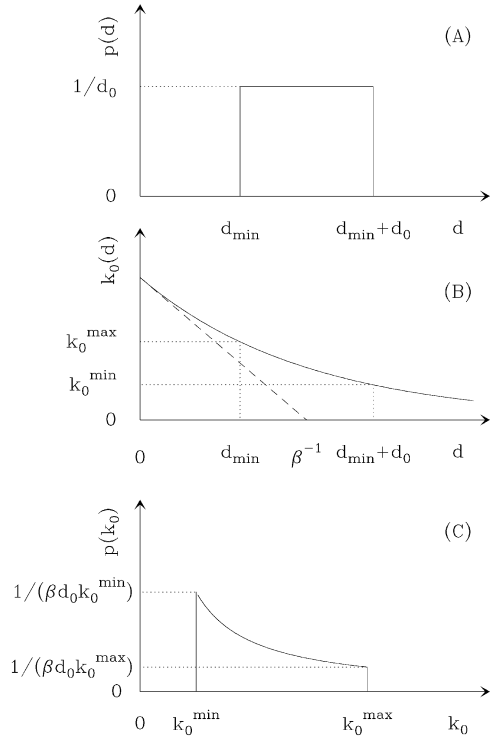

Figure 3. (A) Probability function of *d*, the distance over which tunneling between the electrode surface and the enzyme occurs (eq 4). (B) Dependence of k_0 (the interfacial ET rate constant at zero overpotential) on *d* (eq 3). (C) Resulting probability function of k_0 (eq 5).

on the electrode: this introduces a dispersion of tunneling distances and hence a dispersion of interfacial ET rate constants (Figure 2).

The rate of interfacial ET to the active site decreases exponentially with the tunneling distance *d* between the electrode and the entry point for electrons in the enzyme according to the relationship:

$$k_0(d) = k_0^{\max} \exp(-\beta d) \tag{3}$$

where $k_0^{\max} = k_0^{(d=d_{\min})}$ and β is a decay constant (Figure 3B), the value of which is typically of the order of 1 Å^{-1}. We assume that within a certain range of distances [$d_{\min}$, $d_{\max} = d_{\min} + d_0$], all of the values of *d* occur with the same probability (Figure 3A), i.e.,

$$p(d) = 1/d_0 \text{ for } d \in [d_{\min}, d_{\min} + d_0] \tag{4}$$

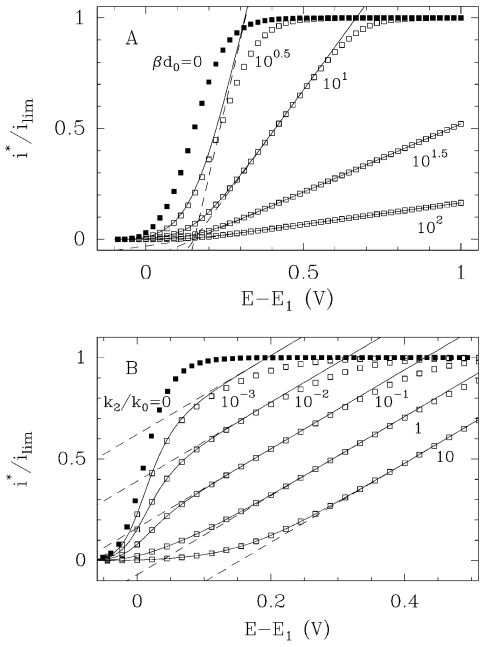

Figure 4. Steady state voltammograms calculated according to eq 6 (empty squares) and approximations given by eqs 8 (plain lines) and 9 (dashed lines) for $E_{O/I} = E_{I/R} = E_1$. (A) $k_2/k_0^{\max} = 10^1$ and from left to right, $\beta d_0 = 10^{0.5}$, 10, $10^{1.5}$, and 10^2 (empty squares); filled symbols, $k_2/k_0^{\max} = 10$ and $\beta d_0 \rightarrow 0$ (eq 2 with $k_2/k_0 = 10$). (B) $\beta d_0 = 10$ and from left to right, $k_2/k_0^{\max} = 10^{-3}$, 10^{-2}, 10^{-1}, 1, and 10. Filled symbols, $k_2/k_0^{\max} \rightarrow 0$ (eq 2 with $k_2/k_0 = 0$).

The square function has been chosen for simplicity, since both the enzyme molecule and the electrode surface at which it is bound have irregular shapes, and further definition is not useful.

Combining the probability function of *d* (eq 4) and the dependence of k_0 on *d* (eq 3), the probability of ET occurring with a given value of k_0 is

$$p(k_0) = \begin{cases} (\beta d_0)^{-1} k_0^{-1} & \text{for } k_0 \in [k_0^{\min}, k_0^{\max}] \\ 0 & \text{for any other value} \end{cases} \tag{5}$$

with $k_0^{\min} = k_0^{\max}\exp(-\beta d_0)$. Equation 5 is derived in the Supporting Information section and is plotted in Figure 3C.

Corrected Waveshape. Starting from an equation for the waveshape as a function of two reduction potentials and the interfacial ET rate at zero overpotential k_0 (eq 2), the current is easily integrated across all possible values of k_0 in the range [$k_0^{\min}$, $k_0^{\max}$] (eq 5). As demonstrated in the Supporting Information section, the corrected current i^* is represented by:

$$\frac{i^*}{i_{\lim}} = \frac{1}{a^{ox}}\left(1 + \frac{1}{\beta d_0}\ln\frac{a^{ox} + b_2^{ox}}{a^{ox} + b_1^{ox}}\right) \tag{6a}$$

$$a^{ox} = 1 + e_{O/I}^{-1}(1 + e_{I/R}^{-1}) \tag{6b}$$

$$b_2^{ox} = \frac{k_2}{k_0^{\max}}(e_{I/R}^{-1/2} + e_{O/I}^{-1/2}(1 + e_{I/R}^{-1})) \tag{6c}$$

$$b_1^{ox} = b_2^{ox}\exp(\beta d_0) \tag{6d}$$

The corresponding equation for catalytic reduction is given in the Supporting Information section.

In Figure 4, eq 6 is plotted as empty squares; the filled symbols are plots of the ideal waveshapes, given by eq 2, and valid when there is no distribution of ET rates or when ET is very fast with respect to turnover number (k_2). Panel A

corresponds to $k_2/k_0^{max} = 10$ and increasing values of βd_0 (from left to right). A large value of βd_0 corresponds to a distribution of tunneling distances (d_0) that is wide with respect to β^{-1}. As βd_0 increases, the number of enzyme molecules having a small value of k_0 increases, and this results in a transition from a sigmoidal wave to a linear current response. If βd_0 is small, k_0^{min} is very close to k_0^{max}, and the effect of the dispersion of tunneling distances is negligible: the limiting case $\beta d_0 \rightarrow 0$ is given by eq 2 and plotted as filled squares in Figure 4A. The departure from ideal behavior when k_2/k_0^{max} increases (for a given value of βd_0) is illustrated in Figure 4B. For small values of k_2/k_0^{max}, the limitation due to interfacial ET is relaxed.

Approximations. When the driving force increases, the last exponential term to vanish in eq 2 is $(k_2/k_0)e_{O/I}^{-1/2}$ or $(k_2/k_0)e_{I/R}^{-1/2}$ depending on which of the reduction potentials ($E_{O/I}$ or $E_{I/R}$) is the greater. To avoid distinguishing this case (and only in the derivation of eqs 7 and 9), we consider hereafter that $E_{O/I} = E_{I/R} = E_1$. For this case, in the high driving force limit (just before the exponential terms vanish), the current eq 2 reduces to

$$\frac{i}{i_{lim}} \approx \frac{1}{1 + \frac{2k_2}{k_0} e_1^{-1/2}} \tag{7}$$

At high driving force, the contribution to the current of a given adsorbed enzyme molecule for which k_0 is small appears around $E = E_1 + (2/f)\ln(2k_2/k_0)$, i.e., it is shifted to a higher driving force by the ET limitation.[26] The linear change in current as a function of electrode potential E, which results from the addition of contributions of all enzyme molecules with a small value of k_0/k_2, is therefore expected for E values lying between $E_1 + (2/f)\ln(2k_2/k_0^{max})$ and $E_1 + (2/f)\ln(2k_2/k_0^{min})$, i.e., over a range of electrode potential $\approx 2RT/F \times \beta d_0$.

For the data shown in Figure 1, the current does not level off in the experimental potential range. This corresponds to $E < E_1 + (2/f)\ln(2k_2/k_0^{min})$, i.e., $b_1^{ox} \gg a^{ox}$. Equation 6a then simplifies to

$$\frac{i^*}{i_{lim}} \approx \frac{1}{\beta d_0\, a^{ox}} \ln \frac{a^{ox} + b_2^{ox}}{b_2^{ox}} \tag{8}$$

with a^{ox} and b_2^{ox} as defined in eq 6b,c. The plot of eq 8 is shown as solid lines in Figure 4 and departs from eq 6 (empty squares) only at high driving force (when the limiting current is reached) or when βd_0 is small (so that the electrode potential range over which the "ohmic" behavior is expected is virtually nonexistent, panel A).

Similarly, the equation for the linear part of the voltammogram at high driving force is given by $a^{ox} \approx 1$ and $b_1^{ox} \gg 1 \gg b_2^{ox}$, so that eq 6 (with $E_{O/I} = E_{I/R} = E_1$) reduces to

$$\frac{i^*}{i_{lim}} \approx \frac{1}{\beta d_0}\left(\frac{f}{2}(E - E_1) - \ln\frac{2k_2}{k_0^{max}}\right) \tag{9}$$

(dashed lines in Figure 4), and the slope of the linear part of the voltammogram is

$$\partial i^*/\partial E = \frac{i_{lim}}{\beta d_0}\frac{F}{2RT} \tag{10}$$

Results

Samples of *A. vinosum* [NiFe]hydrogenase were prepared as described in ref 27, and electrochemical experiments were conducted as described in refs 5, 11, and 12. Voltammograms of catalytic H_2 oxidation by *A. vinosum* [NiFe]hydrogenase adsorbed at a PGE electrode are plotted as empty squares in Figure 5.[28] Comparison with Figure 4B shows that the change in shape as the temperature increases is consistent with a relatively greater increase in enzyme activity as compared to interfacial ET (an increase of k_2 relative to k_0 at constant βd_0).

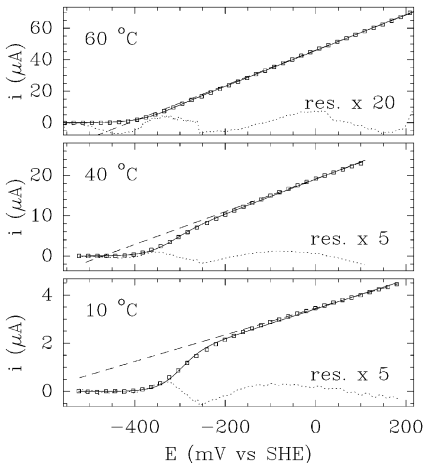

Figure 5. Fits of catalytic voltammograms[28] such as those shown in Figure 1 to eq 8 (plain line, enlarged residues are plotted as dotted lines) and fits of the high potential parts of the voltammograms to straight lines (dashed) according to eq 9.

The fit of the linear, high driving force part of the data to a straight line is also shown in Figure 5 (dashed lines). Equation 10 predicts that the product of the slope times the temperature is proportional to the limiting current and therefore to the activity (this assumes that the coverage of enzyme remains unchanged as the temperature is varied, but see below); however, note that whereas the limiting current cannot be measured from the data in Figure 5, the slope can. Therefore, measuring the slope of the voltammogram is equivalent to measuring the activity of the enzyme. The exponential increase of $(\partial i/\partial E \times T)$ with T is shown in Figure 6A, and the semilog plot in panel B allows the activation energy (E_a) of the catalytic hydrogen oxidation reaction to be measured. The slope of the straight line in Figure 6B equates to $-E_a/R$ and gives $E_a \approx 50$ kJ/mol, a value that is common to many enzymes.

Equation 8 can be used to fit the whole waveshape by adjusting two reduction potentials, k_2/k_0^{max} and $i_{lim}/\beta d_0$. Remarkably, adding a dispersion of ET rate constants to the model does not increase the number of adjustable parameters. The fits of the voltammograms in Figure 1 to eq 8 are shown as plain lines in Figure 5.[29] Because the temperature dependence of k_0 (involving electron tunneling) is much lower than that of k_2 (involving changes in covalent bonding), the change in k_2/k_0^{max} determined by fitting the catalytic voltammograms to eq 8 as a function of T is an additional measure of the temperature dependence of activity. The adjusted value of k_2/k_0^{max} is plotted in Figure 6C and gives $E_a \approx 60$ kJ/mol. This measure of k_2/k_0^{max} is independent of the slope of the voltammograms because, as shown in Figure 4B, changing k_2/k_0^{max} affects the shape of the low driving force part of the voltammogram, whereas the slope is measured at the high potential limit. Therefore, the agreement between the values of E_a deduced from Figure 6B,C is a check of the consistency of the model.

From an experimental point of view, the comparison of the residual slopes of different voltammograms relies on the assumption that the electroactive coverage is unchanged (eq 10 shows that the slope is proportional to i_{lim} and therefore to Γ).

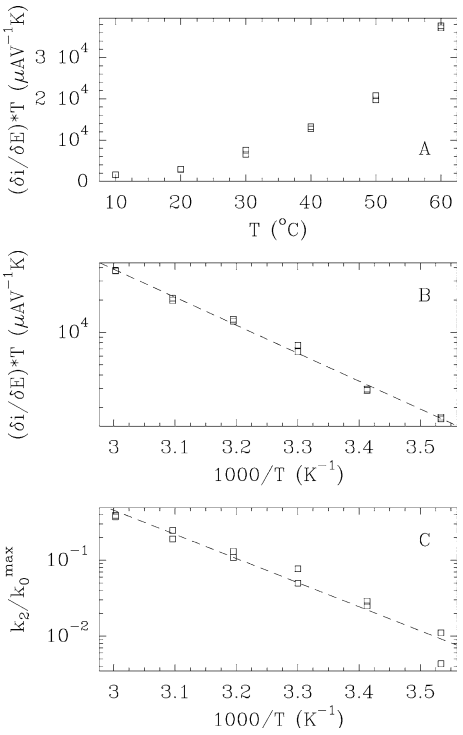

Figure 6. (A) Plot of the high driving force slope of the voltammograms (dashed lines in Figure 5) times the temperature, as a function of the temperature. (B) Semilog plot allowing the activation energy of the H_2 oxidation reaction to be measured from the high driving force slope of the voltammogram. (C) Semilog plot of the value of k_2/k_0^{max} determined by fitting the voltammograms to eq 8 (plain lines in Figure 5).

No such assumption is made when the change in k_2/k_0 is determined by fitting the voltammograms to eq 8, as this parameter characterizes the shape (as opposed to the magnitude) of the signals.

Discussion

When a redox enzyme undergoes direct ET with an electrode, the catalytic voltammograms often show a residual slope over a large range of electrode potential at high driving force (Figure 1), whereas it is simply predicted that it should reach a plateau. This observation, made with many multicentered redox enzymes[3−5,12−20] and with less complex enzymes such as cytochrome *c* peroxidase (Bateman, L.; Goodin, D. B.; Armstrong, F. A. Unpublished results),[30] has not been discussed previously in the context of enzyme electrocatalysis. In this paper, we propose a general model based on the idea that disorder among the adsorbed enzyme molecules (Figure 2) results in a distribution of tunneling distances and thus a dispersion of the interfacial ET rates.

Assuming that the distribution of orientations is such that within a certain range (of width d_0) all of the possible distances between the electrode surface and the entry point for electrons in the enzyme occur with the same probability (eq 4 and Figure 3A), the resulting distribution of k_0 values is given by eq 5 (Figure 3C). The catalytic current corresponding to the heterogeneous assembly of enzymes molecules was derived by averaging over the distribution of interfacial ET rate constants (eq 6), and a linear change in current as a function of electrode potential at high driving force was predicted (eq 9).

In simple terms, this behavior results from the contribution of enzyme molecules having low k_0 values with respect to turnover (k_2), which contribute only at greater driving force. Because it results from competition between turnover and interfacial ET, the linear response should become more prominent as the activity of the enzyme increases. This is indeed the trend observed for hydrogen oxidation by *A. vinosum* [NiFe]-hydrogenase, for which the catalytic signal changes from sigmoidal to linear when the temperature is increased (Figure 1). Notably, this enzyme is extremely active (high k_2), hence the ease with which this effect is observed. Another interesting example comes from the study[20] of the respiratory nitrate reductase from *Paracoccus pantotrophus*. Here, the greater activity for chlorate reduction than for nitrate reduction correlates with a greater residual slope in the voltammogram when chlorate is the substrate.[31] The same effect has also been observed with the nitrate reductase from *Escherichia coli* (Elliot, S. J.; Weiner, J. H.; Blasco, F.; Armstrong, F. A. Unpublished results).

The model developed here can be used to fit the catalytic data for hydrogen evolution and oxidation by *A. vinosum* [NiFe]-hydrogenase over a large range of experimental conditions (temperature and pH). The study of the pH dependence of voltammetry gives insights into the catalytic cycles and is thoroughly discussed in ref 5, whereas here, we have focused on the temperature dependence of the voltammetry. The activation energy of the hydrogen oxidation reaction was estimated from the change of both the high potential slope and the shape of the voltammograms as a function of temperature. The fact that these two independent measurements give similar values for the activation energy ($E_a = 55 \pm 5$ kJ/mol) supports the consistency of the analysis. The model we propose makes it possible to deconvolute intrinsic properties of the active site and film/interfacial ET properties and may be applied to other adsorbed redox enzymes.

The well-defined nature of electrochemical data obtained with adsorbed molecules usually makes deviations from ideal behaviors rather apparent. For noncatalytic systems, local interactions between the redox sites in nearby adsorbed molecules,[32−34] spatial distribution of potentials within the electrode double layer,[35−41] and distribution of ET rate constants exhibited by redox centers in the layer[41−54] have all been suggested to account for nonideal peak widths or separations.[55] In order for the electrochemical data to depend on the properties of interfacial ET, the system must be driven far from equilibrium; this is usually achieved by using transient techniques, such as fast-scan cyclic voltammetry or chronoamperometry. It is important to note that in the present study, steady-state experiments reveal the nonideal properties of interfacial ET; this is because the catalytic reaction competes continuously with the redox transformation of the active site following ET.

Increasingly inclined plateau currents can be observed when a redox process at a rotating disk electrode involves an adsorbed catalyst (see ref 56 and references therein). To explain these observations, Jiang and Anson proposed a model based on a wide, Gaussian distribution of reduction potentials of the catalyst−substrate complex.[56] To test which nonidealities could explain the results in Figure 1, we performed (numerical) integrations of the ideal current eq 2 with a distribution of several parameters: Gaussian (i.e., normal) distribution of reduction potentials and normal, log-normal, and uniform distributions of distances between the electrode and the electron acceptor. In all cases, this broadens the catalytic wave, but no distribution apart from that used in the model presented here was found to result in the linear shape seen in Figure 1.

The observations presented in this paper may suggest how electron transport catalysis in real biological systems would be affected in situations where the subunits of an enzyme complex

are not connected together in a single, well-defined manner, exemplified by the complexes between myoglobin and cytochrome b_5[57,58] and plastocyanin and cytochrome *c*.[59]

In a recent paper, reporting how the electrocatalytic oxidation of H_2 by *A. vinosum* hydrogenase compares with that of a Pt-coated electrode, we identified less than ideal interfacial ET as a possible shortcoming of the enzyme system.[12] We can now see that ET is not uniformly limiting but that efforts to achieve greater homogeneous high values of k_0 may well provide an important improvement in the performance of enzymes as electrocatalysts, for example, in the development of hydrogenases as future biofuel cell catalysts.

Acknowledgment. We thank W. Roseboom for preparing the purified *A. vinosum* enzyme, B. Audit (European Bioinformatics Institute, Cambridge, U.K.), V. Guirardel (Department of Mathematics, Université Joseph Fourier, Grenoble, F.), P. N. Bartlett (Department of Chemistry, University of Southampton, U.K.), and J. P. McEvoy (Inorganic Chemistry Laboratory, Oxford) for invaluable discussions. This work was supported by funds from the UK EPSRC and BBSRC (Grant Nos. 43/B10492 and 43/E16711) and The Netherlands Organization for Scientific Research (NWO) division for Chemical Science (CW). A.K.J. thanks the Rhodes Trust and the NSF for scholarships.

Supporting Information Available: Derivation of eqs 5 and 6 and corresponding equation for a reductive wave. This material is available free of charge via the Internet at http://pubs.acs.org.

References and Notes

(1) Armstrong, F. A.; Heering, H. A.; Hirst, J. *Chem. Soc. Rev.* **1997**, *26*, 169−179.

(2) Page, C. C.; Moser, C. C.; Chen, X.; Dutton, P. L. *Nature* **1999**, *402*, 47−52.

(3) Heffron, K.; Léger, C.; Rothery, R. A.; Weiner, J. H.; Armstrong, F. A. *Biochemistry* **2001**, *40*, 3117−3126.

(4) Léger, C.; Heffron, K.; Pershad, H. R.; Maklashina, E.; Luna-Chavez, C.; Cecchini, G.; Ackrell, B. A. C.; Armstrong, F. A. *Biochemistry* **2001**, *40*, 11234−11245.

(5) Léger, C.; Jones, A. K.; Roseboom, W.; Albracht, S. P. J.; Armstrong., F. A. *Biochemistry* **2002**, in press.

(6) Cammack, R., Frey, M., Robson, R., Eds. *Hydrogen as a Fuel, Learning from Nature*; Taylor and Francis: London and New York, 2001.

(7) Maroney, M. J.; Bryngelson, P. A. *J. Biol. Inorg. Chem.* **2001**, *6*, 453−459.

(8) Siegbahn, P. E. M.; Blomberg, M. R. A.; Wirstam, M.; Crabtree, R. H. *J. Biol. Inorg. Chem.* **2001**, *6*, 460−466.

(9) Fan, H.-J.; Hall, M. B. *J. Biol. Inorg. Chem.* **2001**, *6*, 467−473.

(10) Bertrand, P.; Dole, F.; Asso, M.; Guigliarelli, B. *J. Biol. Inorg. Chem.* **2000**, *5*, 682−691.

(11) Pershad, H. R.; Duff, J. L. C.; Heering, H. A.; Duin, E. C.; Albracht, S. P. J.; Armstrong, F. A. *Biochemistry* **1999**, *38*, 8992−8999.

(12) Jones, A. K.; Sillery, E.; Albracht, S. P. J.; Armstrong, F. A. *Chem. Commun.* **2002**, 866−867.

(13) Bianco, P.; Haladjian, J. *J. Electrochem. Soc.* **1992**, *139*, 2428−2432.

(14) Butt, J. N.; Filipiak, M.; Hagen, W. R. *Eur. J. Biochem.* **1997**, *245*, 116−122.

(15) Sucheta, A.; Cammack, R.; Weiner, J.; Armstrong, F. A. *Biochemistry* **1993**, *32*, 5455−5465.

(16) Sucheta, A.; Ackrell, B. A. C.; Cochran, B.; Armstrong, F. A. *Nature* **1992**, *356*, 361−362.

(17) Hirst, J.; Sucheta, A.; Ackrell, B. A. C.; Armstrong, F. A. *J. Am. Chem. Soc.* **1996**, *118*, 5031−5038.

(18) Hirst, J.; Ackrell, B. A. C.; Armstrong, F. A. *J. Am. Chem. Soc.* **1997**, *119*, 7434−7439.

(19) Butt, J. N.; Thornton, J.; Richardson, D. J.; Dobbin, P. S. *Biophys. J.* **2000**, *78*, 1001−1009.

(20) Anderson, L. J.; Richardson, D. J.; Butt, J. N. *Biochemistry* **2001**, *40*, 11294−11307.

(21) Bard, A. J.; Faulkner, L. R. *Electrochemical Methods. Fundamentals and Applications*, 2nd ed.; John Wiley & Sons: New York, 2001.

(22) Heering, H. A.; Hirst, J.; Armstrong, F. A. *J. Phys. Chem. B* **1998**, *102*, 6889−6902.

(23) Chidsey, C. E. D. *Science* **1991**, *251*, 919−922.

(24) Two distinct apparent k_2/k_0 parameters, corresponding to each of the ET steps, should appear in eq 2 (see ref 5). From the point of view of data analysis, this increases the number of adjustable parameters without resulting in better fits to the data. Therefore, we make hereafter the assumption that these two parameters have the same value.

(25) Volbeda, A.; Charon, M. H.; Piras, C.; Hatchikian, E. C.; Frey, M.; Fontecilla-Camps, J. C. *Nature* **1995**, *373*, 580−587.

(26) Bond, A. M. *Modern Polarographic Methods in Analytical Electrochemistry*; Marcel Dekker: New York, 1980.

(27) Coremans, J.; van Garderen, C. J.; Albracht, S. P. J. *Biochim. Biophys. Acta* **1992**, *1119*, 148−156.

(28) A linear baseline (dotted line in Figure 1), extrapolated from the potential range where the faradaic current is zero, was subtracted to remove the contribution from the capacitive current.

(29) When the voltammograms were fit to eq 8, the adjusted value of $E_{I/R}$ was systematically found to lie below the potential range where a catalytic current is measured. This implies that the value of this reduction potential cannot be determined from the catalytic voltammograms. Therefore, to fit the data, we used modified versions of eq 6b,c, where the terms $e_{I/R}{}^{-1}$ and $e_{I/R}{}^{-1/2}$ were fixed to zero, leaving three adjustable parameters ($E_{O/I}$, $k_2/k_0{}^{max}$, and $i_{lim}/\beta d_0$).

(30) The fact that nonwired enzymes—for which direct interfacial ET occurs from the electrode to the active site—also show this behavior makes unlikely the hypothesis that it results from an electric field effect on the rate of intramolecular ET (as opposed to interfacial ET).

(31) Anderson, L. J. Thesis, University of East Anglia, 2002.

(32) Albery, W. J.; Boutelle, M. G.; Colby, P. J.; Hillman, A. R. *J. Electroanal. Chem.* **1982**, *133*, 135−145.

(33) Laviron, E. *Electroanal. Chem. Interfacial Electrochem.* **1974**, *52*, 395−402.

(34) Brown, A. P.; Anson, F. C. *Anal. Chem.* **1977**, *49*, 1589−1595.

(35) Smith, C. P.; White, H. S. *Anal. Chem.* **1992**, *64*, 2398−2405.

(36) Lecomte, S.; Hildebrandt, P.; Soulimane, T. *J. Phys. Chem. B* **1999**, *103*, 10053−10064.

(37) Andreu, R.; Calvente, J. J.; Fawcett, W. R.; Molero, M. *Langmuir* **1997**, *13*, 5189−5196.

(38) Calvente, J. J.; Andreu, R.; Molero, M.; Lopez-Perez, G.; Dominguez, M. *J. Phys. Chem. B* **2001**, *105*, 9557−9568.

(39) Honeychurch, M. J. *Langmuir* **1998**, *14*, 6291−6296.

(40) Gerischer, H.; Scherson, D. A. *J. Electroanal. Chem.* **1985**, *188*, 33−38.

(41) Pilloud, D. L.; Chen, X. X.; Dutton, P. L.; Moser, C. C. *J. Phys. Chem. B* **2000**, *104*, 2868−2877.

(42) Albery, W. J.; Bartlett, P. N.; Wilde, C. P.; Darwent, J. R. *J. Am. Chem. Soc.* **1985**, *107*, 1854−1858.

(43) Creager, S. E.; Wooster, T. T. *Anal. Chem.* **1998**, *70*, 4257−4263.

(44) Tender, L.; Carter, M. T.; Murray, R. W. *Anal. Chem.* **1994**, *66*, 3173−3181.

(45) Weber, K.; Creager, S. E. *Anal. Chem.* **1994**, *66*, 3164−3172.

(46) Richardson, J. N.; Rowe, G. K.; Carter, M. T.; Tender, L. M.; Curtin, L. S.; Peck, S. R.; Murray, R. W. *Electrochim. Acta* **1995**, *40*, 1331−1338.

(47) Ingram, R. S.; Murray, R. W. *J. Chem. Soc., Faraday Trans.* **1996**, *92*, 3941−3946.

(48) Carter, M. T.; Rowe, G. K.; Richardson, J. N.; Tender, L. M.; Terrill, R. H.; Murray, R. W. *J. Am. Chem. Soc.* **1995**, *117*, 2896−2899.

(49) Brevnov, D. A.; Finklea, H. O.; Van Ryswyk, H. *J. Electroanal. Chem.* **2001**, *500*, 100−107.

(50) Finklea, H. O.; Hanshew, D. D. *J. Am. Chem. Soc.* **1992**, *114*, 3173−3181.

(51) Katz, E.; Willner, I. *Langmuir* **1997**, *13*, 3364−3373.

(52) Rowe, G. K.; Carter, M. T.; Richardson, J. N.; Murray, R. W. *Langmuir* **1995**, *11*, 1797−1806.

(53) Nahir, T. M.; Bowden, E. F. *J. Electroanal. Chem.* **1996**, *410*, 9−13.

(54) Li, J. H.; Schuler, K.; Creager, S. E. *J. Electrochem. Soc.* **2000**, *147*, 4584−4588.

(55) In the literature, normal[52,53] distributions of distances between the electrode and the redox center and log-normal distribution of ET rates[42] have been considered. Although a uniform distribution of distances was recently proposed,[54] the corresponding distribution of k_0 values (eq 5) was not explicitly derived.

(56) Jiang, R. Z.; Anson, F. C. *J. Electroanal. Chem.* **1991**, *305*, 171−184.

(57) Worrall, J. A. R.; Liu, Y.; Crowley, P. B.; Nocek, J. M.; Hoffman, B. M.; Ubbink, M. *Biochemistry* **2002**, *41*, 11721−11730.

(58) Liang, Z.-X.; Jiang, M.; Ning, Q.; Hoffman, B. M. *J. Biol. Inorg. Chem.* **2002**, *7*, 580−588.

(59) Ubbink, M.; Bendall, D. S. *Biochemistry* **1997**, *36*, 6326−6335.